Effects of textured journal bearings on vibrations of lightweight rotors

J. Rebufa, E. Le Guyadec, D. Mazuyer, F. Thouverez

Effects of textured journal bearings on vibrations of lightweight rotors

J. Rebufa[1, 2], E. Le Guyadec[1], D. Mazuyer[2], F.Thouverez[2]
[1]CEA, Commissariat à l'énergie atomique et aux énergies alternatives, DEN - DTEC 30200 Bagnols sur Cèze, France
[2]LTDS, Laboratoire de Tribologie et de Dynamique des Systèmes, Ecole Centrale de Lyon, 69130 Ecully, France

ABSTRACT
A dynamic model of a rotating shaft on two textured hydrodynamic bearings is presented. The hydrodynamic mean pressure is computed using multi-scale periodic homogenization and is projected on a flexible shaft with internal damping. The steady state solutions of an unbalance response are analysed with two sinusoidal texturing patterns. The stability zone and the amplitude of limit cycle are presented. The harmonic balance method applied to the monolithic resolution of the fluid structure coupling is efficient and allows parametric studies of stability.

Keywords: Textured bearings, Multi-scale homogenization, Non-linear rotor dynamics

1 INTRODUCTION

Advanced rotating machineries, using small rotors or working at high rotating speeds, require a complete control of the vibration components. Lubrication systems, such as hydrodynamic journal bearings play a crucial role in the dynamical behaviour of the whole machinery and have a significant influence on structures vibrations. Predictions of the shaft vibrations are complex due to the nonlinear behaviour of the hydrodynamic bearing. Dynamic coefficients of bearings ([1]) are widely used for computing the stability of equilibrium points. Nevertheless, they do not take into account non-linear effects of the bearings, that may lead to unstable motion ([2], [3], [4]).
Furthermore, cavitation in the lubricant appears and changes drastically the pressure distribution. Several cavitation models could be retained leading in most cases to different behaviours. The recent adaptation of the Reynolds cavitation model ([4]) and the Jacobson-Floberg-Olsson ([5]) to a linear complementary problem is straightforward and efficient.
Besides, recent improvements in surface texturing have shown several enhancements in hydrodynamic lubrication such as friction reduction or improvement of drag force ([6]). One of the first study suggesting that micro irregularities could improve the lubrication has been made almost 50 years ago by Hamilton ([7]). Several studies have been following in order to model the surface state influence with its statistical properties ([8], [9]). Among them Patir and Cheng introduced the idea of averaging the Reynolds equation by introducing the flow factors method. Elrod has been one of the first to apply the perturbation method with multiple-scale analysis to Reynolds equation ([10]). The homogenization of Reynolds equation has been mathematically formalized by Bayada *et al.* with mass conservation model of cavitation ([11], [12]) and has also been developed recently in a transient form and a compressible form by Almqvist *et al.* ([13], [14]). In these models the assumptions of Reynolds equation need to

be verified at the two different scales. Many works have been devoted to analyse the validity of the Reynolds equation in presence of surface texturing as reported De Kraker *et al.* in [15]. In their article they adapted the flow factor method with a local CFD computation. The improvement of the computing power also allowed several deterministic static study of the bearing ([16], [17]). However, to consider the surface effects in a numerical analysis a very fine mesh is needed leading to prohibitive computational time in a dynamic analysis. Homogenization techniques provide a rigorous way of averaging the influence of a periodic texturing pattern. One can study the influence of a micro scale texturing pattern on the macro scale with a relatively coarse mesh, and take into account the average pressure distribution and cavitation zone. Eventually, the mean pressure profile can be projected on the structure at each time step to study the dynamics of the shaft lubricated by two textured bearings.
Effects of the texturing pattern on the dynamic behaviour of the system are not well known and need to be properly analysed. So far, few works have been devoted on the stability and transient analysis of the journal bearing with roughness effect ([18],[19],[20]). The resulting dynamic system is complex and efficient motion studies must be used to allow parametric analysis of surface texturing influence. The Harmonic Balance Method (HBM) is an efficient tool for periodic solution research. To convert in the frequency domain complex nonlinearities such as hydrodynamic bearing resultant force the Alternate Frequency/Time domain method (AFT) is efficient and widely used in rotor dynamic systems ([21], [22], [23]). Moreover, the algebraic expression of the motion equation in the frequency domain allows substantial reduction of the problem to nonlinear degrees of freedom ([24]).
In this study we present a homogenized model taking into account a periodic texturing pattern on a rotating flexible shaft. A monolithic system is presented where mass conserving cavitation and surface texturing are taken into account in the finite hydrodynamic bearing model. The HBM/AFT method with interface reduction is used to study the vibration amplitude of the unbalance response and the stability of limit cycles. The particular cases of longitudinal and transverse sinusoidal texturing will be studied.

2 FLUID FILM FORCE COMPUTATION WITH HOMOGENIZATION TECHNIQUE

The Reynolds equation with mass conservation algorithm is often used in hydrodynamic lubrication in its isoviscous and unstationary form ([13], [14]):

$$\frac{\partial}{\partial x}\left(\frac{h^3}{12\,\mu}\frac{\partial p}{\partial x}\right)+\frac{\partial}{\partial y}\left(\frac{h^3}{12\,\mu}\frac{\partial p}{\partial y}\right)=\frac{R\Omega}{2}\frac{\partial \theta h}{\partial x}+\frac{\partial \theta h}{\partial t}$$
$$p\mathrm{r}=0\ ,\quad p\geq 0\ ,\quad \mathrm{r}\geq 0$$

In this equation p is the pressure relative to the cavitation pressure, usually different from the ambient pressure, h describes the film height, μ the lubricant viscosity, R the shaft radius, Ω the shaft rotating velocity. Like in the Elrod algorithm ([25]) the film is viewed as a mixture and θ represents the relative mixture density. The relative motion of the shaft is in the x direction, and y represents the transverse direction to the flow.
In order to take into account a small variation of amplitude, one can decompose the film height with the plain bearing height h_0 and the periodic local height due to the texturing pattern $h_{\xi\zeta}$

$$h(x,y,\xi,\zeta)=h_0(x,y)+h_{\xi\zeta}(\xi,\zeta) \qquad (1)$$

Coming from the idea of separating the two different scales, the film height can be expressed

$$h_\epsilon(x,y) = h\left(x, y, \frac{x}{\epsilon}, \frac{y}{\epsilon}\right) \tag{2}$$

The main idea of multiple scales method relies on the asymptotic expansion of the solution

$$p = p_0 + \epsilon p_1 + \epsilon^2 p_2 + \cdots \tag{3}$$

With these assumptions the homogenized problem is to find the pressure p_0 solution to the homogenized problem. The expressions of the coefficients A_{ij} and B_i are available in the general case in several articles ([12], [13]). In this paper we make the assumptions that the film height can be decomposed in the following form:

$$h(x, y\,, x\epsilon, y\epsilon) = h_1(\theta, y, \theta\epsilon)\; h_2(\theta, y, y\epsilon) \tag{4}$$

With these assumptions the coefficient expressions are available in [12] :

$$A_{11} = \frac{\widetilde{h_2^3}}{\widetilde{h_1^{-3}}}, \qquad A_{22} = \frac{\widetilde{h_1^3}}{\widetilde{h_2^{-3}}} \quad , \quad A_{12} = A_{21} = 0$$

$$B_1 = \frac{\widetilde{h_1^{-2}}}{\widetilde{h_1^{-3}}}\;\widetilde{h_2}\,, \qquad B_2 = 0 \quad , \qquad \Theta = \frac{1}{\widetilde{h_2}\widetilde{h_1^{-2}}}\left(\frac{\widetilde{\theta_0 h_2}}{\widetilde{h_1^2}}\right)$$

Where $\tilde{\cdot}$ represents the average operator. The homogenized Reynolds equation in that case is

$$\frac{\partial}{\partial x}\left(\frac{A_{11}}{12\mu}\frac{\partial p_0}{\partial x}\right) + \frac{\partial}{\partial y}\left(\frac{A_{22}}{12\mu}\frac{\partial p_0}{\partial y}\right) = \frac{R\Omega}{2}\frac{\partial \Theta B_1}{\partial x} + \frac{\partial \Theta h_0}{\partial t} \tag{5}$$

Table 1 – Homogenized factors for transverse and longitudinal sinusoidal texturing

	Transverse	Longitudinal
$h\_\epsilon(x,y,x\epsilon,y\epsilon)$	$h(x,y) + h_r \sin(x\epsilon)$	$h(x,y) + h_r \sin(y\epsilon)$
$A_{11}(x,y)$	$2\frac{(h(x,y)^2 - h_r^2)^{\frac{5}{2}}}{2\,h(x,y)^2 + h_r^2}$	$h(x,y)^3 + \frac{3}{2}h(x,y)h_r^2$
$A_{22}(x,y)$	$h(x,y)^3 + \frac{3}{2}h(x,y)h_r^2$	$2\frac{(h(x,y)^2 - h_r^2)^{\frac{5}{2}}}{2\,h(x,y)^2 + h_r^2}$
$B_1(x,y)$	$\frac{2h(x,y)(h(x,y)^2 - h_r^2)}{2h(x,y)^2 + h_r^2}$	$h(x,y)$

In the case when only one surface is textured it is possible to simplify the problem to a stationary problem ([13]). The film height is also independent of which side is textured due to Reynolds hypothesis. In order to compute the mean pressure distribution the finite element method can be used ([5]). Moreover the problem can be written as a linear complementary problem ([4], [5]). The discretized problem can be written then

$$\begin{cases} \mathbb{H}(\mathbf{x})\,\bar{\mathbf{p}} \;+\; \mathbb{Q}\,\bar{\mathbf{r}} = \mathbf{f}_{\mathrm{f}}(\mathbf{x}) \\ \bar{\mathbf{p}}^{\mathrm{T}}\,\bar{\mathbf{r}} = 0 \;\;,\;\; \bar{\mathbf{p}} \geq 0 \;\;,\;\; \bar{\mathbf{r}} \geq 0 \end{cases} \tag{6}$$

where $\bar{\mathbf{p}}$ represents the dimensionless discrete pressure vector and $\mathbf{x}$ the shaft displacements vector.

The dimensionless pressure is obtained with the following formula: $\bar{p} = \frac{p}{12\mu\Omega\left(\frac{R}{C}\right)^2}$

The boundary conditions in this study are only the atmospheric value of pressure at the bearing edge. As there is no supply groove, the rotating frame is even easier to program for the bearing pressure computation because the fluid grid is moving.
Depending of the choice of the cavitation model (Reynolds or JFO), the matrix $\mathbb{Q}$ can be either the identity matrix ([4]) or the mass conservation matrix ([5]).
The matrix $\mathbb{H}$ and the vector $\mathrm{f_f}$ are expressed:

$$\mathbb{H}_{ij}(\mathbf{x}) = \int_\Gamma \left[A_{11}(h)\frac{\partial W_i}{\partial x}\frac{\partial N_{f_j}}{\partial x} + \frac{R^2}{L^2}A_{22}(h)\frac{\partial W_i}{\partial y}\frac{\partial N_{f_j}}{\partial y}\right] d\Gamma$$

$$\mathbf{f}_{\mathrm{f}_i}(\mathbf{x}) = -\frac{1}{2}\int_\Gamma W_i \frac{\partial B_1(h)}{\partial x}\, d\Gamma$$

W_i and N_{f_j} state for the test function and the interpolation function of the finite element method, respectively. However, the $\mathbb{H}$ matrix and $\mathbf{f}_\mathrm{f}$ vector are non-linearly dependent of the shaft position. For each new position of the journal the matrix coefficient must be computed with the integration of the flow factors. In order to compute efficiently the matrix $\mathbb{H}(\mathbf{x})$ and the vector $\mathrm{f_f}(\mathbf{x})$ for each time step of the solver method, a polynomial development of the homogenized factor is used. The algorithm allows also the tilt of the shaft in the bearing. For example, one can write the average film height with a misaligned shaft in the pure squeeze rotating coordinates ([26]):

$$h = 1 + e_1 y\cos(2\pi x) + e_2(1-y)\cos(2\pi x)$$

where e_1 and e_2 are the eccentricity of the two bearing edges.

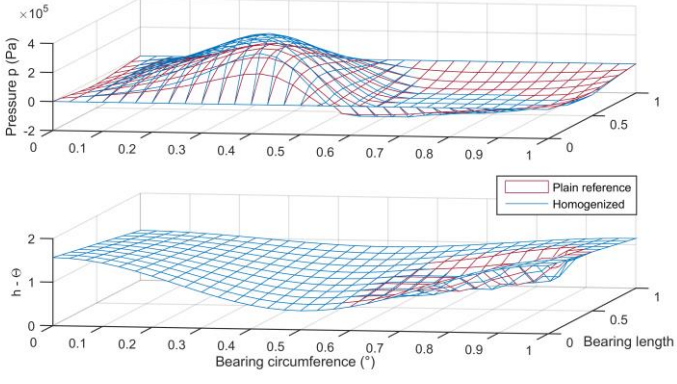

Figure 1 – Homogenized pressure profile with sinusoidal longitudinal pattern with $h_r = 0.4\,C_r$ with the bearing parameter of table 2 with tilted shaft the relative eccentricity $e_1 = 0.4$, $e_2 = 0.1$

A polynomial approximation of $A_{11}(h)$ at the order 3 is taken: $A_{11}(h) = \sum_{n=0}^{3}\alpha_n h^n$ and $A_{22}(h) = \sum_{n=0}^{3}\beta_n h^n$.
From the trinomial expansion we obtain:

$$(1+\epsilon_1 y\cos(x) + \epsilon_2(1-y)\cos(x))^{\mathrm{n}} = \sum_{0\le j\le k\le n}\left[\frac{\mathrm{n!}}{(\mathrm{n-k})!\,(\mathrm{k-j})!\,\mathrm{j!}}\right] e_1^{k-j} y^{k-j} e_2^j (1-y)^j\ \cos^k(x)$$

Thus if we note

$$[a_{pq}]_{ij} = \int_\Gamma y^p (1-y)^q \cos^{p+q}(x) \frac{\partial W_i}{\partial x} \frac{\partial N_{f_j}}{\partial x} \, d\Gamma \quad , \quad [b_{pq}]_{ij} = \int_\Gamma y^p (1-y)^q \cos^{p+q}(x) \frac{\partial W_i}{\partial y} \frac{\partial N_{f_j}}{\partial y} \, d\Gamma$$

We have then

$$\mathbb{H}_{ij} = \sum_{0 \le j \le k \le n \le 3} \left[\frac{\mathrm{n!}}{(\mathrm{n-k})!\,(\mathrm{k-j})!\,\mathrm{j!}} \right] \left(\alpha_n a_{(k-j)j} + \frac{R^2}{L^2} \beta_n b_{(k-j)j} \right) e_1^{k-j} e_2^j$$

As the 10 matrices b_{pq} and d_{pq} are computed at the program initialization the assembly of the matrix $\mathbb{H}_{ij}$ is efficient. The same idea is easily applied to assemble $\mathbf{f}_\mathrm{f}$.

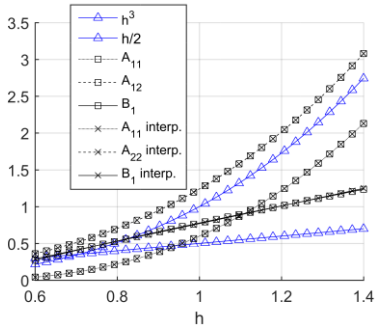

Figure 2 - Polynomial interpolation of flow factors for transverse texturing pattern

3 A MONOLITHIC PROBLEM

3.1 A Rotordynamic system of a shaft on two bearings

The journal is modelled by a Timoshenko beam. A viscoelastic constitutive equation is taken ([27]):

$$\sigma = E(\epsilon + \eta\dot{\epsilon}) \tag{7}$$

Where σ and ϵ are the main component of the stress tensor and the strain tensor in the beam neutral axis direction, respectively. Only the viscous damping is modelled, the hysteretic damping is taken equal to zero. The dynamic equation of a rotor with internal damping at constant rotating velocity is:

$$\mathbb{M}\ddot{\mathbf{x}} + [\mathbb{K}_b + \Omega\mathbb{G}]\dot{\mathbf{x}} + [\mathbb{K} + \Omega\mathbb{K}_c]\mathbf{x} = \mathbf{f}_\mathrm{d}(\Omega) + \mathbf{f}_\mathrm{s} + \mathbf{f}_\mathrm{b} \tag{8}$$

where $\mathbb{M}$, $\mathbb{G}$, $\mathbb{K}$, $\mathbb{K}_b$, $\mathbb{K}_c$, $\mathbf{f}_\mathrm{s}$, and $\mathbf{f}_\mathrm{d}$, are the mass matrix, gyroscopic matrix, stiffness matrix, structural damping matrix, circulatory matrix, static load force vector, and unbalance force vector, respectively. The gyroscopic matrix $\mathbb{G}$ arises from the rotating movement of the Timoshenko beam. The circulatory matrix comes from the elastic deformation of the rotating beam with the viscoelastic law ([27]). With the constitutive law (7) the damping matrix is directly related to the stiffness matrix: $\mathbb{K}_b = \eta\mathbb{K}$. The discretised displacement vector $\mathbf{x}$ is made of 4 degrees of freedom per node ([27]). In order to project the fluid pressure on the structure one can express the virtual work of the bearings pressure on the shaft:

$$\delta W = \int_0^L \int_0^{2\pi} (\cos(\theta)\,\delta u + \sin(\theta)\,\delta w)\, p\, R\, d\theta\, dy \tag{9}$$

As the inertia forces are neglected in Reynolds equation the choice of the pressure grid can be made in the rotating frame ([26]).

After discretization:

$$\delta W = \delta \mathbf{x}^{\mathrm{T}} \mathbb{P} \mathbf{p} \tag{10}$$

The matrix $\mathbb{P}$ is constructed directly from the fluid interpolation functions and the structure test functions.

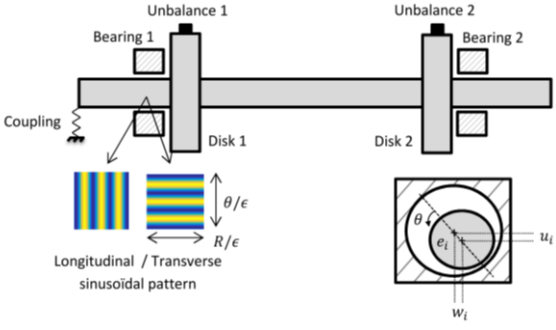

Figure 3 - Rotor - bearing system configuration

This allows taking into account the tilt of the shaft in the bearing. Hence, the dynamic system of equation of the system becomes

$$\begin{cases} \mathbb{M}\ddot{\mathbf{x}} + [\mathbb{K}_b + \Omega\mathbb{G}]\dot{\mathbf{x}} + [\mathbb{K} + \Omega\mathbb{K}_c]\mathbf{x} = \mathbf{f}_{\mathrm{d}}(\Omega) + \mathbf{f}_{\mathrm{s}} + \mathbb{P}\bar{\mathbf{p}} \\ \mathbb{H}(\mathbf{x})\,\bar{\mathbf{p}} \;+\; \mathbb{Q}\,\bar{\mathbf{r}} = \mathbf{f}_{\mathrm{f}}(\mathbf{x}) \\ \bar{\mathbf{p}}^{\mathrm{T}}\,\bar{\mathbf{r}} = 0 \;\;,\;\; \bar{\mathbf{p}} \geq 0 \;\;,\;\;\; \bar{\mathbf{r}} \geq 0 \end{cases} \tag{11}$$

3.2 Application of the Harmonic Balance Method

The HBM consists in a search of solution of the form of a truncated Fourier series:

$$x = X_0 + \sum_{n=1}^{N_h} \mathrm{X_{nc}}\cos(n\omega t) + X_{ns}\sin(n\omega t) \tag{12}$$

Introducing the following notations

$$X = \left[X_0\ \mathrm{X_{nc}}\ \mathrm{X_{nc}} \ldots \mathrm{X_{nc}}\ \mathrm{X_{N_hc}}\right]^T \tag{13}$$

$$T = [I\ \cos(\omega t)\, I\ \ \sin(\omega t)\, I\ \ \ldots\ \ \cos(n\omega t)\, I\ \ \ \sin(n\omega t)\, I\ ]^T$$

$$\nabla = diag(0_{n\times n}\ \nabla_1 \ldots \nabla_{\mathrm{N_h}}) \quad \text{with} \quad \nabla_{\mathrm{k}} = k\begin{bmatrix} 0 & I \\ -I & 0 \end{bmatrix}$$

leads to the expression of the displacement, velocity and acceleration with the frequency domain unknowns vector:

$$x = TX \qquad \dot{x} = \omega\, T\nabla X \qquad \ddot{x} = \omega T\nabla^2 X \tag{14}$$

By replacing these expressions in (11) and after a projection on the trigonometric functions basis one obtain a new nonlinear system without any time dependence:

$$(\omega^2 N_M + \omega N_C + N_k)X = F + F_{NL}(X) \tag{15}$$

with $N_M = diag(M, \ldots, M)$ a block diagonal matrix of $2N_h + 1$ blocks, N_C and N_K are constructed identically with the matrices $[\mathbb{K}_b + \Omega\mathbb{G}]$ and $[\mathbb{K} + \Omega\mathbb{K}_c]$, respectively.

The force F is composed by the static and dynamics load on their respective trigonometric projection.
The F_{NL} represents the non-linear projection in the frequency domain. To compute this vector, the Alternate Frequency/Time domain has been used ([21]). From the frequency unknown vector X, the position and velocity are constructed from equation (14). Then the fluid model allows us to compute the resulting force in the time domain from solving equation (8) and projecting the pressure with the projection matrix in (10). A Discrete Fourier Transform (DFT) of the resulting discrete time vector leads to the contribution of the non-linear force on each harmonic. This method can be resumed by the following scheme:

$$X \xrightarrow{T} (x, \dot{x}) \rightarrow f_{nl}(\Omega, x, \dot{x}) \xrightarrow{FFT} F_{nl}(X)$$

A basic Newton-Raphson algorithm is used to solve the system (15). Once the solution X the system (15) is found the velocity and displacement in the time domain are reconstructed with equations (14). Then, a stability analysis is performed. There are many ways to perform such an analysis with the HBM ([28]). In this paper we used the exponentials method to compute the monodromy matrix. The Floquet multipliers, i.e. the eigenvalue of the monodromy matrix are then used to analyse stability of the synchronous motion. An unstable limit cycle is characterized by at one Floquet multiplier with a complex modulus greater than 1 ([29]).

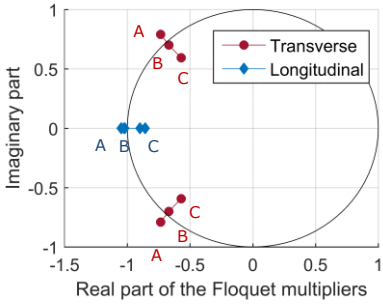

Figure 4 - Neimark-Sacker and period-doubling bifurcation of limit cycles with shaft rotating speed variation for transverse texturing and period doubling bifurcation for longitudinal texturing pattern $h_r = 0.5\ C_r$

4 NON-LINEAR RESPONSE TO MASS UNBALANCE

For a given rotating speed one can consider the stability zone of the unbalance response. The parameters of the study are given in table 2. The only static load applied to the horizontal rotor is its weight. In that case a study of a perfectly balanced shaft leads to highly unstable motions. Van de Vorst *et al.* showed that for lightweight rotors the mass unbalance can achieve stability of the motion ([3]). Besides in the case where the cavitation pressure is sub-ambient, the full film lubrication can happen when the pressure is not low enough for the fluid to vaporize in the bearing. The Sommerfeld pressure profile is thus obtained and leads to highly unstable motions. Adding mass unbalance can solve the problem by forcing cavitation. Although the mass unbalance distribution stabilizes the system, it also increases the amplitude of stable vibration. The aim of this paper is to analyse the impact of surface texturing on the minimum mass unbalance to achieve stability.

Table 2 - Rotor-bearing parameters

Shaft parameters		**Hydrodynamic bearings parameters**	
Radius	$R = 2.5\ mm$	Bearing length	$L_p = 5\ mm$
Young Modulus	$E = 211\ GPa$	Radial clearance	$C_r = 10\ \mu m$
Poisson coefficient	$\nu = 0.3$	Oil viscosity	$\mu = 0.002\ Pa.s$
Density	$\rho_s = 7800\ kg/m^3$	Cavitation pressure	$p_{cav} = -1\ bar$
Shaft length	$L_a = 130\ mm$	**Disks parameters**	
Internal damping coef.	$\eta = 2.10^{-7}$	Density	$\rho_d = 2700\ kg/m^3$
Coupling radial stiffness	$8400\ N/m$	Radius	$R = 7.5\ mm$
Coupling angular stiffness	$0.014\ N/°$	Length	$L_D = 5\ mm$
Rotating velocity range	$2.500 - 3.000\ rad/s$ ~$23.900 - 28.600\ rpm$		

We also focus on the minimum stable vibration amplitude that can be obtained with a certain texturing pattern. Numerical integration shows that the Neimark-Sacker and the flip bifurcation point seem to be subcritical. The minimum mass unbalance to achieve stability for a certain shaft rotating velocity is plotted on the figure 5. For computational time purpose, the Reynolds cavitation hypothesis has been used to solve Reynolds equation in that example. A straightforward dichotomy method has been used to find the Neimark-Sacker bifurcation point.
The computation of Floquet multipliers shows that varying the mass unbalance parameter give rise to a generalized Hopf bifurcation or Neimark-Sacker bifurcation (figure 4) in the case of sinusoidal transverse texturing. In the case of sinusoidal longitudinal texturing as well as for plain bearings the parameters of the study give rise to a flip bifurcation.

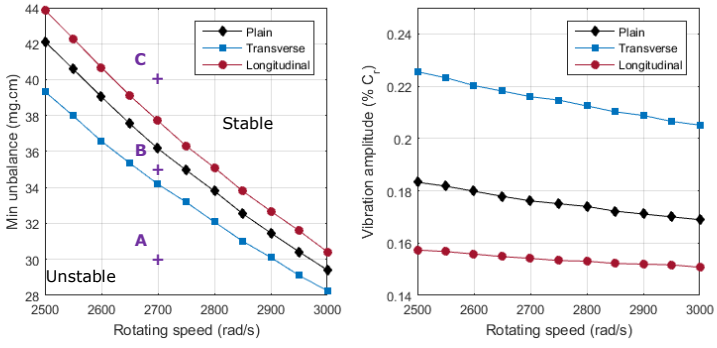

Figure 5 - Minimum mass unbalance for stable motion and vibration amplitude of the corresponding boundary stable system $h_r = 0.5\ C_r$ for each rotating speed

For both systems the minimum unbalance decreases while the rotating speed increases. This means that the system can be unstable during the start-up and stabilise himself after a certain threshold speed. On the diagram we can notice that the minimum unbalance mass is slightly lower for transverse texturing. For example at 2500 rad/s the mass unbalance needed to stabilize the system with sinusoidal transverse texturing (hr = 0.5) is 10% lower than with the sinusoidal longitudinal texturing (hr = 0.5). However, if we pay attention to the vibration amplitude obtained with the boundary stable system we notice that the amplitude value with transverse texturing is 30% higher than with longitudinal texturing.
Figure 6 shows the vibration amplitude with the limit unbalance for stable motion, for different amplitude of sinusoidal texturing patterns. The shaft rotating speed is 2500 rad/s for all the simulation points. The diagram clearly shows the decrease of

vibration amplitude with longitudinal texturing patterns, while with transverse texturing patterns it significantly increases for $h_r \geq 0.1\, C_r$. Below this value we notice a significant variation of the minimum unbalance. For transverse sinusoidal texturing pattern with $h_r \approx 0.1\, C_r$, both the decrease of the minimum unbalance and the vibration amplitude are achieved.

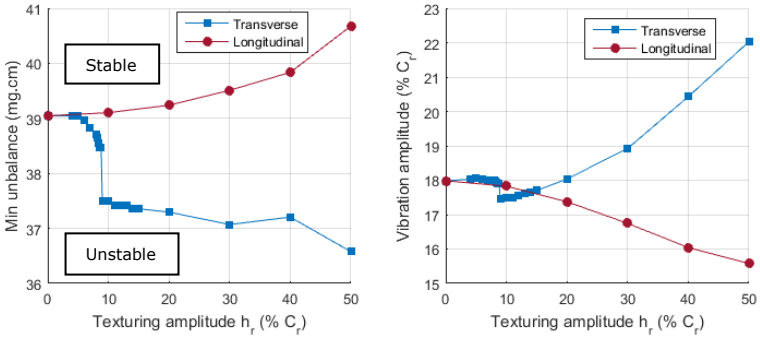

Figure 6 – Vibration amplitude as a function of texturing pattern amplitude for transverse and longitudinal sinusoidal texturing at 2500 rad/s

5 CONCLUSIONS

This study is focused on the impact of textured bearing on small rotating shafts vibration. We have presented a powerful method to study the stability of the unbalance response on the system based on multi-scale homogenization of Reynolds equation. The monolithic resolution of the coupled system of equation is performed. The harmonic balance method gives fast and accurate results to study unbalance response and stability of limit cycles.

We noticed that transverse texturing patterns lower the minimum mass unbalance needed for stability although it increases the vibration amplitude. On the opposite the longitudinal texturing pattern allows substantial reduction of the vibration amplitude. However it increases the minimum unbalance needed for stable motion.

This study has been performed for one dimensional sinusoidal texturing of finite bearing. However, homogenized flow factor for arbitrary textured bearing could be computed and approximated by polynomials separately and added to the algorithm. Furthermore, the algorithm can be adapted for the averaged flow factors of De Kraker ([15]) to take into account recirculation of lubricant in the asperities.

BIBLIOGRAPHY

[1] J. W. Lund, "Review of the Concept of Dynamic Coefficients for Fluid Film Journal Bearings," *J. Tribol.*, vol. 109, no. 1, pp. 37–41, Jan. 1987.

[2] C. J. Myers, "Bifurcation Theory Applied to Oil Whirl in Plain Cylindrical Journal Bearings," *J. Appl. Mech.*, vol. 51, no. 2, pp. 244–250, Jun. 1984.

[3] E. L. B. V. D. Vorst, R. H. B. Fey, A. D. Kraker, and D. H. V. Campen, "Steady-state behaviour of flexible rotordynamic systems with oil journal bearings," *Nonlinear Dyn.*, vol. 11, no. 3, pp. 295–313, Nov. 1996.

[4] T. Zheng and N. Hasebe, "Nonlinear Dynamic Behaviors of a Complex Rotor-Bearing System," *J. Appl. Mech.*, vol. 67, no. 3, pp. 485–495, Nov. 1999.

[5] M. Giacopini, M. T. Fowell, D. Dini, and A. Strozzi, "A Mass-Conserving Complementarity Formulation to Study Lubricant Films in the Presence of Cavitation," *J. Tribol.*, vol. 132, no. 4, pp. 041702–041702, Sep. 2010.

[6] I. Etsion, "State of the Art in Laser Surface Texturing," *J. Tribol.*, vol. 127, no. 1, p. 248, 2005.

[7] D. B. Hamilton, J. A. Walowit, and C. M. Allen, "A Theory of Lubrication by Microirregularities," *J. Basic Eng.*, vol. 88, no. 1, pp. 177–185, Mar. 1966.
[8] S. T. Tzeng and E. Saibel, "Surface Roughness Effect on Slider Bearing Lubrication," *E Trans.*, vol. 10, no. 3, pp. 334–348, Jan. 1967.
[9] N. Patir and H. S. Cheng, "An Average Flow Model for Determining Effects of Three-Dimensional Roughness on Partial Hydrodynamic Lubrication," *J. Tribol.*, vol. 100, no. 1, pp. 12–17, Jan. 1978.
[10] H. G. Elrod, "A General Theory for Laminar Lubrication With Reynolds Roughness," *J. Tribol.*, vol. 101, no. 1, pp. 8–14, Jan. 1979.
[11] G. Bayada and J. B. Faure, "A Double Scale Analysis Approach of the Reynolds Roughness Comments and Application to the Journal Bearing," *J. Tribol.*, vol. 111, no. 2, pp. 323–330, Apr. 1989.
[12] G. Bayada, S. Martin, and C. Vázquez, "An Average Flow Model of the Reynolds Roughness Including a Mass-Flow Preserving Cavitation Model," *J. Tribol.*, vol. 127, no. 4, pp. 793–802, May 2005.
[13] A. Almqvist, E. K. Essel, L.-E. Persson, and P. Wall, "Homogenization of the unstationary incompressible Reynolds equation," *Tribol. Int.*, vol. 40, no. 9, pp. 1344–1350, Sep. 2007.
[14] A. Almqvist, J. Fabricius, and P. Wall, "Homogenization of a Reynolds equation describing compressible flow," *J. Math. Anal. Appl.*, vol. 390, no. 2, pp. 456–471, 2012.
[15] A. de Kraker, R. A. J. van Ostayen, and D. J. Rixen, "Development of a texture averaged Reynolds equation," *Tribol. Int.*, vol. 43, no. 11, pp. 2100–2109, Nov. 2010.
[16] N. Tala-Ighil, M. Fillon, and P. Maspeyrot, "Effect of textured area on the performances of a hydrodynamic journal bearing," *Tribol. Int.*, vol. 44, no. 3, pp. 211–219, Mar. 2011.
[17] V. Brizmer and Y. Kligerman, "A Laser Surface Textured Journal Bearing," *J. Tribol.*, vol. 134, no. 3, pp. 031702–031702, Jun. 2012.
[18] J. Ramesh and B. C. Majumdar, "Stability of Rough Journal Bearings Using Nonlinear Transient Method," *J. Tribol.*, vol. 117, no. 4, pp. 691–695, Oct. 1995.
[19] R. Turaga, A. S. Sekhar, and B. C. Majumdar, "Non-Linear Transient Stability Analysis of a Rigid Rotor Supported on Hydrodynamic Journal Bearings with Rough Surfaces," *Tribol. Trans.*, vol. 43, no. 3, pp. 447–452, Jan. 2000.
[20] J.-R. Lin, "Application of the Hopf bifurcation theory to limit cycle prediction of short journal bearings with isotropic roughness effects," *Proc. Inst. Mech. Eng. Part J J. Eng. Tribol.*, vol. 221, no. 8, pp. 869–879, 2007.
[21] T. M. Cameron and J. H. Griffin, "An Alternating Frequency/Time Domain Method for Calculating the Steady-State Response of Nonlinear Dynamic Systems," *J. Appl. Mech.*, vol. 56, no. 1, pp. 149–154, Mar. 1989.
[22] E. Sarrouy and F. Thouverez, "Global search of non-linear systems periodic solutions: A rotordynamics application," *Mech. Syst. Signal Process.*, vol. 24, no. 6, pp. 1799–1813, Aug. 2010.
[23] A. Grolet and F. Thouverez, "Computing multiple periodic solutions of nonlinear vibration problems using the harmonic balance method and Groebner bases," *Mech. Syst. Signal Process.*, vol. 52–53, pp. 529–547, Feb. 2015.
[24] S. Nacivet, C. Pierre, F. Thouverez, and L. Jezequel, "A dynamic Lagrangian frequency–time method for the vibration of dry-friction-damped systems," *J. Sound Vib.*, vol. 265, no. 1, pp. 201–219, Jul. 2003.
[25] H. G. Elrod, "A Cavitation Algorithm," *J. Tribol.*, vol. 103, no. 3, pp. 350–354, Jul. 1981.
[26] D. Childs, H. Moes, and H. van Leeuwen, "Journal Bearing Impedance Descriptions for Rotordynamic Applications," *J. Lubr. Technol.*, vol. 99, no. 2, pp. 198–210, Apr. 1977.
[27] E. S. Zorzi and H. D. Nelson, "Finite Element Simulation of Rotor-Bearing Systems With Internal Damping," *J. Eng. Power*, vol. 99, no. 1, pp. 71–76, Jan. 1977.
[28] L. Peletan, S. Baguet, M. Torkhani, and G. Jacquet-Richardet, "A comparison of stability computational methods for periodic solution of nonlinear problems with application to rotordynamics," *Nonlinear Dyn.*, vol. 72, no. 3, pp. 671–682, Jan. 2013.
[29] A. H. Nayfeh, *Applied nonlinear dynamics: analytical, computational, and experimental methods*. New York: Wiley, 1995.